# The accurate magnetic structure of $CeAl_2$ at various temperatures in the ordered state



2008 J. Phys.: Condens. Matter 20 135204

(http://iopscience.iop.org/0953-8984/20/13/135204)

J. Phys.: Condens. Matter **20** (2008) 135204 (7pp) doi:10.1088/0953-8984/20/13/135204

# The accurate magnetic structure of $CeAl_2$ at various temperatures in the ordered state

**J Schweizer[1], F Givord[2], J-X Boucherle[2,3], F Bourdarot and E Ressouche**

CEA-Grenoble, DSM/INAC/SPSMS/MDN, 38054 Grenoble Cedex 9, France

E-mail: jacques.schweizer@cea.fr

Received 9 January 2008, in final form 13 February 2008
Published 7 March 2008
Online at stacks.iop.org/JPhysCM/20/135204

**Abstract**

The magnetic structure of the cubic compound $CeAl_2$ is incommensurate and double-$\boldsymbol{k}$. The moments on the two Ce sites describe two elliptical helices of opposed chiralities and lie in the $(1\bar{1}0)$ plane, with their Fourier components $\boldsymbol{m}^k$ close to the [111] direction. Recent symmetry considerations, including for the first time the inversion center of the crystal, have reduced the number of parameters of this structure and have underlined the existence of a phase difference between the projections $m_x^k$, $m_y^k$ and $m_z^k$ of $\boldsymbol{m}^k$. Up to now, although many neutron investigations have been carried out on $CeAl_2$ single crystals, no set of magnetic intensities was available which was large and good enough to check whether this phase difference exists or not.

We have measured such a set of data, taking great care of the instrumental resolution in order to avoid unwanted contributions to the intensities from other domains. As the magnetic form factor of the $\Gamma_7$ ground state of $CeAl_2$ depends very much on the direction of the applied field, it was necessary to go through a self-consistent determination of the magnetic form factor in the direction of the Fourier components $\boldsymbol{m}^k$ to obtain good agreement between the refined magnetic structure and the experimental data. The resulting Fourier components are close but not exactly along the [111] direction and their departure from this direction at low temperature reduces the ellipticity of the helices. The phase difference between the projections $m_x^k$, $m_y^k$ and $m_z^k$ is small but undoubtedly exists and is temperature dependent. It leads to a small distortion of the elliptical helices, with magnetic moments slightly out of the $(1\bar{1}0)$ plane.

(Some figures in this article are in colour only in the electronic version)

## 1. Introduction

$CeAl_2$ is a Kondo compound which orders antiferromagnetically at low temperature. Very few compounds have undergone as many steps for a complete determination of their magnetic structure. It has been constantly studied for 30 years by neutron scattering, with more and more sophisticated investigation methods. During this period, group theory analyses first confirmed the compatibility of the proposed magnetic structures with the crystal symmetry, and then added more details to be checked experimentally. It is the aim of this paper to give an answer to these latter propositions.

$CeAl_2$ crystallizes in the fcc Laves phase, with two Ce atoms in the primitive unit cell, $Ce_1$ and $Ce_2$ in $\pm(1/8, 1/8, 1/8)$ along one diagonal of the cube, at the same positions as the carbon atoms in the diamond structure (figure 1). A first neutron diffraction experiment made on a $CeAl_2$ powder established the appearance of magnetic lines below $T_N = 3.8$ K. These lines, though very faint, were indexed with a propagation vector $\boldsymbol{k} = (1/2 + \delta, 1/2 - \delta, 1/2)$, with $\delta = 0.112$, which means an antiferromagnetic structure along the [111] diagonal, propagating sinusoidally along a direction $[1\bar{1}0]$, perpendicular to the former one. The

[1] Author to whom any correspondence should be addressed.
[2] CNRS staff.
[3] Present address: dr11, CNRS, BP166, 38042 Grenoble Cedex 9, France.

 

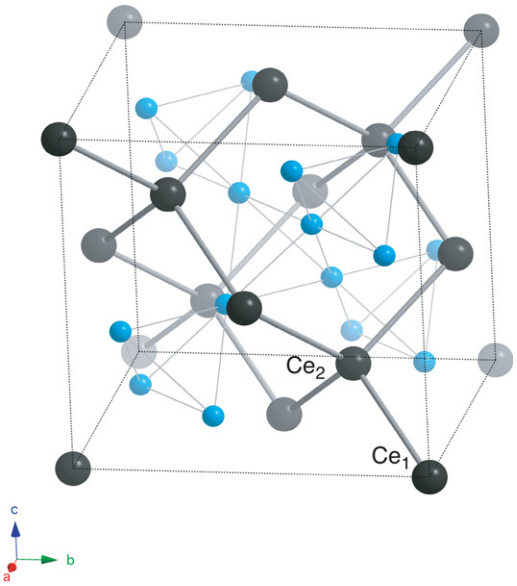


**Figure 1.** Crystal structure of $CeAl_2$. For a better comprehension of the figure, the cell has been translated by (1/8, 1/8, 18).

treatment of the magnetic intensities led to a structure where the moments of the two Ce neighbors $Ce_1$ and $Ce_2$, on the same [111] diagonal, are equal and opposed to each other. The Fourier components $\boldsymbol{m}_1^k$ and $\boldsymbol{m}_2^k$ which are associated with their magnetic moments $\boldsymbol{m}_1(\boldsymbol{l})$ and $\boldsymbol{m}_2(\boldsymbol{l})$ in the cell labeled $\boldsymbol{l}$ through the relation

$$\boldsymbol{m}_j(\boldsymbol{l}) = \sum_k \boldsymbol{m}_j^k \mathrm{e}^{-2\mathrm{i}\pi \boldsymbol{k}\cdot\boldsymbol{l}} + \mathrm{cc} \tag{1}$$

are aligned along the [111] diagonal of the cube [1]. Later, a spherical polarization analysis experiment on a single crystal (neutron diffraction polarization analysis in the three dimensions) came to the result that the Fourier components are not exactly aligned along the diagonal of the cube and that the deviation from this direction keeps increasing when the temperature decreases below $T_N$ [2].

Attempts to check whether this structure is single-$\boldsymbol{k}$ or multi-$\boldsymbol{k}$ were also undertaken. By applying successively uniaxial pressure and magnetic field aligned along the [11$\bar{2}$] direction of the crystal, Barbara *et al* [3, 4] ruled out the triple-$\boldsymbol{k}$ structure suggested by [5]. Then Forgan *et al* [6], observing the intensity changes when a magnetic field is applied far from the symmetry axes of the crystal, proved unambiguously that the structure is double-$\boldsymbol{k}$: two propagation vectors of the type $\boldsymbol{k}_1 = (1/2 + \delta, 1/2 - \delta, 1/2)$ and $\boldsymbol{k}_2 = (1/2 + \delta, 1/2 - \delta, -1/2)$ are coupled. These equivalent propagation vectors share the same sinusoidal part $(\delta, -\delta, 0)$, the part which is superimposed on two different antiferromagnetic propagation vectors: $(1/2, 1/2, 1/2)$ and $(1/2, 1/2, -1/2)$. As is well known, the phase between the two Fourier vectors $\boldsymbol{m}^{k_1}$ and $\boldsymbol{m}^{k_2}$ cannot be determined by experiment. The authors proposed a $\pi/2$ phase as being the phase most compatible with the fact that $Ce^{3+}$ is a Kramers ion, which, in principle, should have a constant moment at low temperature. Actually, the $\pi/2$ phase provides for the two sites elliptical helices of opposed chiralities instead of sinusoids. As a matter of fact, helices are more suitable than sinusoids for a Kramers ion as its moment cannot be reduced to zero at very low temperature. Arguing on free energy considerations, Harris *et al* [7] agreed with this $\pi/2$ phase.

In the meantime, group theory analyses figured out the relations which are imposed by the symmetry operators (crystal symmetries and propagation vector symmetries) on the Fourier components $m_{j\alpha}^k$ and $m_{j\beta}^k$ ($\alpha$ and $\beta$ for the components $x$, $y$ and $z$ of atoms $Ce_1$ and $Ce_2$). The usual representation analysis, conserving in the little group $G_k$ only the operators which keep the propagation vector unchanged, led to the following relations [8]:

$$\begin{aligned} m_{1x}^k &= m_x^k & m_{2x}^k &= -m_{1y}^k \\ m_{1y}^k &= m_y^k & m_{2y}^k &= -m_{1x}^k \\ m_{1z}^k &= m_z^k & m_{2z}^k &= -m_{1z}^k. \end{aligned} \tag{2}$$

The magnetic structures which were deduced from the experiments were compatible with these relations, with the experimental extra relations $m_x^k = m_y^k = m_z^k$ for [1] and $m_x^k = m_y^k$ for [2]. The relations (2) are often considered as defining a magnetic structure depending only on three parameters: $m_x^k$, $m_y^k$, $m_z^k$. But one has to keep in mind that these parameters are complex, which means that such a structure is actually defined by five quantities: three lengths and two phases, the third phase being defined arbitrarily.

A recent theoretical investigation [9, 10] included the inversion operator $\boldsymbol{I}$ in the symmetry analysis. In particular, in terms of group theory, it associated the operator $\boldsymbol{I}$ with the conjugation operator $\boldsymbol{C}$ in the little group $G_k$. Each of these operators changes $\boldsymbol{k}$ in $-\boldsymbol{k}$, but their product keeps the propagation vector unchanged. This corepresentation analysis brought more constraints than the former representation analysis: a constraint on the lengths (the $x$ and $y$ components of the moments must have equal lengths), and a constraint on the phases:

$$\begin{aligned} m_{1x}^k &= |m_x^k|\mathrm{e}^{\mathrm{i}\varphi} & m_{2x}^k &= -|m_x^k|\mathrm{e}^{-\mathrm{i}\varphi} = -m_{1y}^k \\ m_{1y}^k &= |m_x^k|\mathrm{e}^{-\mathrm{i}\varphi} & m_{2y}^k &= -|m_x^k|\mathrm{e}^{\mathrm{i}\varphi} = -m_{1x}^k \\ m_{1z}^k &= |m_z^k| & m_{2z}^k &= -|m_z^k| = -m_{1z}^k \end{aligned} \tag{3}$$

where $|m_x^k|$ and $|m_z^k|$ are real quantities. Only three parameters remain to characterize the magnetic structure, among them a phase $\varphi$ which was not, up to now, taken into account by the experimentalists.

At this point, it was realized that though a large number of neutron investigations have been performed on this compound, no single crystal data collection was available, large enough and good enough to check whether this phase $\varphi$ exists or not. We have decided to measure such a good quality data set. The aim of this paper is to describe this experiment, to present the final magnetic structure of $CeAl_2$ as it has been obtained from these data and the way the different structural parameters of the ordered magnetic structure (lengths and phase) change with temperature.

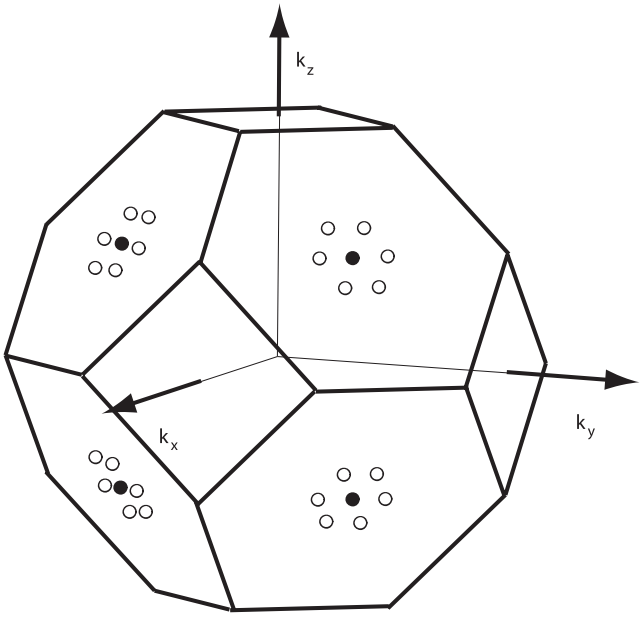


**Figure 2.** First Brillouin zone of $CeAl_2$.

## 2. Experimental details and results

### *2.1. The magnetic domains and the star of vectors* $\boldsymbol{k}$*: an experimental problem*

The magnetic reflections obtained from a single crystal arise from different magnetic domains in relation to the number of equivalent $\boldsymbol{k}$ vectors, that is the star of $\boldsymbol{k}$. The vector $\boldsymbol{k} = (1/2+\delta, 1/2-\delta, 1/2)$ lies on the first Brillouin zone boundary and may be decomposed in a sum $(1/2, 1/2, 1/2)+(\delta, -\delta, 0)$. There are eight possibilities for the direction $(1/2, 1/2, 1/2)$, and for each of them, six possibilities for a direction $(\delta, -\delta, 0)$ perpendicular to $(1/2, 1/2, 1/2)$. Altogether, there are then 48 vectors but 24 of them can be deduced from the 24 others by a translation of type $(1, 1, 1)$, a vector of the reciprocal lattice. We can then say that the star of vector $\boldsymbol{k}$ contains 24 vectors, although there are 48 vectors at the surface of the Brillouin zone. The magnetic reflections are located on small hexagons around each position $(h \pm 1/2, k \pm 1/2, l \pm 1/2)$ of the reciprocal space which are the centers of the eight hexagonal faces of the Brillouin zone (figure 2). As $\delta$ is very small ($\delta = 0.112$), the hexagons are very narrow and it is a delicate operation to measure the integrated intensity of one of the magnetic spots without it being contaminated by the others. As will be seen in the following, great care has to be taken.

Magnetic domains of type K are present. As vectors $\boldsymbol{k}$ and $-\boldsymbol{k}$ are associated in the same domain, the number of domains is half the number of vectors of the star of $\boldsymbol{k}$, that is 12 domains K in the case of a single-$\boldsymbol{k}$ structure. For a multi-$\boldsymbol{k}$ structure, different vectors $\boldsymbol{k}$ are coupled together to form one magnetic domain and their number is reduced consequently: for instance for this double-$\boldsymbol{k}$ structure, six magnetic domains remain.

### *2.2. A first experiment on D15*

A first experiment was performed on the single crystal diffractometer D15 at ILL (Grenoble, France). This instrument is a diffractometer with a lifting detector arm, located on an inclined thermal beam, on which the wavelength is fixed and equal to 1.17 Å. The $CeAl_2$ sample was a crystal of dimensions $7 \times 6 \times 5$ mm$^3$, mounted with its axis $[1\bar{1}0]$ vertical. It was installed in an orange cryostat able to go down to a temperature as low as 1.25 K.

We collected two sets of magnetic reflections at two temperatures: 1.25 K and 2.95 K. The first set consisted of reflections of type $(h \pm (1/2 \pm \delta), k \pm 1/2, l \pm (-1/2 \pm \delta))$ while the second set was composed of reflections $(h \pm (1/2 \pm \delta), k \mp 1/2, l \pm (-1/2 \pm \delta))$. In both collections, the associated nuclear reflections $(hkl)$ were mainly in the horizontal plane, that is of type $(hhl)$. The rocking curves of several magnetic reflections appeared to be non-single peaks, indicating that the resolution of the instrument was not tight enough to measure one of the six spots of the hexagon without being contaminated by the others.

### *2.3. A second experiment on D23*

After the failure of the first experiment, we performed a second experiment on the diffractometer D23, which is located on one of the thermal guides of the ILL and which is also a diffractometer with a lifting detector arm. We measured the same $CeAl_2$ crystal, with the same axis $[1\bar{1}0]$ vertical, but we optimized the resolution conditions:

(i) we chose a wavelength of 2.376 Å, double the former one,
(ii) we measured reflections of type $(h \pm (1/2+\delta), k \pm (1/2-\delta), l \pm 1/2)$, with also most of the $(hkl)$ reflections in the horizontal plane.

With this choice of wavelength the angular separations between the magnetic satellites in the hexagons were about twice as large as in the D15 experiment. We checked, by different scans, and particularly by scanning the lifting detector angle $\nu$, that the measurement of one of the magnetic spots did not include contributions from any of the five other spots of the same hexagon. At three temperatures, 1.3, 2.6 and 3.5 K, we measured the integrated intensities of 60 of these magnetic spots. Once the intensities of the Friedel pairs had been averaged, this number went down to 32.

### *2.4. Structure refinements of the D23 measurements*

The magnetic intensity $I(\boldsymbol{\kappa} = \boldsymbol{H} \pm \boldsymbol{k})$ for a reflection $(hkl)^{\pm}$ corresponding to the reciprocal vector $\boldsymbol{H} = (hkl)$ is:

$$I(\boldsymbol{\kappa} = \boldsymbol{H} \pm \boldsymbol{k}) = \boldsymbol{F}_{M\perp}(\boldsymbol{\kappa}) \cdot \boldsymbol{F}^{*}_{M\perp}(\boldsymbol{\kappa}) \cdot \delta(\boldsymbol{\kappa} - \boldsymbol{H} \mp \boldsymbol{k}) \quad (4)$$

where $\boldsymbol{F}_{M\perp}(\boldsymbol{\kappa})$ is the projection of the magnetic structure factor $\boldsymbol{F}_M(\boldsymbol{\kappa})$ on the plane perpendicular to $\boldsymbol{\kappa}$, and $\boldsymbol{F}_M(\boldsymbol{\kappa})$ is expressed as a function of the Fourier components $\boldsymbol{m}^k_j$ of the atom $j$ as:

$$\boldsymbol{F}_M(\boldsymbol{\kappa}) = \sum_j \boldsymbol{m}^k_j f_j(\boldsymbol{\kappa}) \cdot \mathrm{e}^{2\mathrm{i}\pi\boldsymbol{\kappa}\cdot\boldsymbol{r}_j}. \quad (5)$$

**Table 1.** Ratio $|m_z^k|/|m_x^k|$ and phase $\varphi$ deduced from the structure refinements at various temperatures $T$. $\theta_H$ and $\theta_{m^k}$ are the angles of the applied field $H$ and the Fourier component $\boldsymbol{m}^k$ with the [111] direction. The reliability factor is defined as $R = \sqrt{\sum_i p_i (I_i^{\rm obs} - I_i^{\rm calc})^2 / \sum_i p_i (I_i^{\rm obs})^2}$ and $\chi^2 = \sum_i p_i (I_i^{\rm obs} - I_i^{\rm calc})^2 / (N_{\rm obs} - N_{\rm var})$ with $p_i = 1/\sigma_i^2$.

| $T$ (K) | f | $R$ | $\chi^2$ | $\varphi$ (deg) | $\lvert m_z^k\rvert/\lvert m_x^k\rvert$ | $\theta_{m^k}$ (deg) | $\theta_H$ (deg) |
|---|---|---|---|---|---|---|---|
| 1.30 | dip. | 21.3% | 29.8 | =0 | 0.993(0.054) | −0.20(1.46) | — |
| 1.30 | calc. | 7.04% | 3.25 | =0 | 1.046(0.015) | 1.22(0.40) | 1.20 |
| 1.30 | calc. | 6.93% | 3.27 | −1.21(1.06) | 1.044(0.016) | 1.18(0.41) | 1.15 |
| 2.68 | dip. | 19.2% | 22.1 | =0 | 0.958(0.044) | −1.16(1.24) | — |
| 2.68 | calc. | 7.73% | 3.59 | =0 | 1.024(0.016) | 0.65(0.43) | 0.65 |
| 2.68 | calc. | 7.71% | 3.69 | −0.62(1.25) | 1.023(0.017) | 0.63(0.44) | 0.65 |
| 3.52 | dip. | 13.2% | 11.6 | =0 | 0.929(0.029) | −1.97(0.82) | — |
| 3.52 | calc. | 6.46% | 2.78 | =0 | 0.989(0.014) | −0.29(0.38) | −0.28 |
| 3.52 | calc. | 5.89% | 2.38 | 3.9(1.4) | 0.988(0.013) | −0.33(0.35) | −0.32 |

$f_j(\boldsymbol{\kappa})$ is the magnetic form factor associated with the atom $j$. As mentioned in section 1, the Fourier components $\boldsymbol{m}_1^k$ and $\boldsymbol{m}_2^k$ for the two Ce atoms satisfy the relations (3) and depend on the three parameters $|m_x^k|$, $|m_z^k|$ and $\varphi$.

We have refined the ratio $|m_z^k|/|m_x^k|$ and $\varphi$ using the program MXD [11]. The absolute values of $|m_z^k|$ and $|m_x^k|$ could not be determined separately because of strong extinction on the nuclear reflections. The previous experiment on powder had led to a value of $|m_z^k| = |m_x^k| = 0.44 \pm 0.05\ \mu_{\rm B}$. At first, the values used for $f_j(\boldsymbol{\kappa})$ were given by the isotropic dipolar form factor $\langle j_0\rangle + c_2\langle j_2\rangle$ of the $Ce^{3+}$ ion ($c_2 = 1.6$) [12, 13]. The reliability factors $R$ at the three temperatures are fairly bad, ranging between 13% and 21% (see table 1). The agreement is so bad that refining the value of $\varphi$ was unreasonable and its value was fixed to zero. We noticed that among the 32 measured reflections, about 1/3 of them presented systematic discrepancies, which could not be attributed to measuring uncertainties: reflections calculated as equal were in fact observed equal but with intensities which did not fit the model. This feature suggested to us that the magnetic form factor that we used was inadequate.

As a matter of fact, previous polarized neutron diffraction studies have evidenced very unusual form factors for the $Ce^{3+}$ ion of $CeAl_2$ [14]. These investigations were carried out in the paramagnetic state, with a magnetic field applied either along the two-fold or the four-fold axis. The striking aspect of the form factor is the extreme scattering of the experimental points, particularly when the field was along the two-fold axis. In our experiment, the direction of $\boldsymbol{m}_j^k$ being close to the [111] direction, we calculated the magnetic form factor for each measured reflection with a three-fold reference axis (see appendix A) using the wavefunctions of the different levels. These were obtained by diagonalizing the Hamiltonian of the system, which is the sum of crystal electric field and Zeeman terms. The crystal field Hamiltonian depends only on the parameter $B_4 = 0.29$ K (corresponding to a splitting of 100 K [15]). We assumed no exchange contribution and a field of 1 T applied in the plane $(1\bar{1}0)$ at a small angle $\theta_H$ from [111].

As the Fourier component is not exactly along [111], the refinement process was performed in a self-consistent way until the final direction of $\boldsymbol{m}^k$ is the same as the direction of the applied field taken to calculate the form factor used in the refinement ($\theta_{m^k} = \theta_H$). The final form factor, which is very sensitive to the direction of the applied field, is very slightly sensitive to its value. It is compared to the dipolar value in figure 3 and one can notice that it is now very anisotropic with large deviations from the dipolar values for most reflections. Results of the refinements at the three temperatures are shown in table 1. The reliability factors are much better. Refining the phase parameter $\varphi$ also improves the refinements and the values of all parameters are given in table 1. The calculated intensities are compared to the observed ones at the lowest temperature $T = 1.3$ K in table 2.

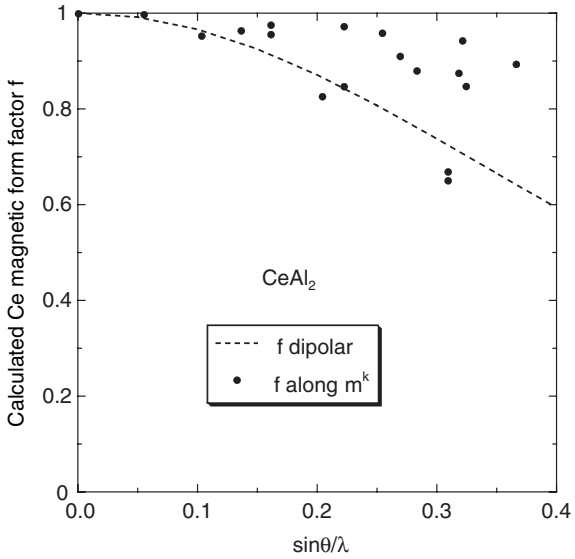


**Figure 3.** Calculated cerium magnetic form factor in $CeAl_2$ for an applied field at $\theta_H = 1.15°$ from the three-fold axis [111]. The dotted line is the dipolar spherical form factor.

The value of the ratio $|m_z^k|/|m_x^k|$ determines the ellipticity $e$ of the helices: the moment amplitude varies between $|m_x^k|\sqrt{2}$ in the $(x, y)$ plane and $|m_z^k|$ along the $z$ direction. As temperature decreases, the ellipticity is reduced from $e = 1.43$ at 3.52 K to $e = 1.35$ at 1.30 K, the moments thus varying a little less.

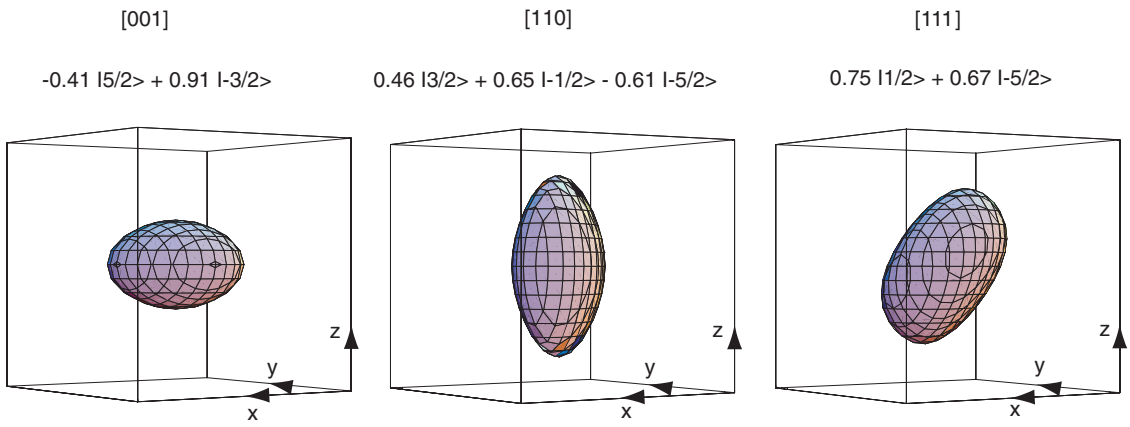


**Figure 4.** Magnetic densities for an infinitesimal field applied along the four-fold, two-fold and three-fold axes. To emphasize the asymmetrical part of the magnetization, we have subtracted the spherical density corresponding to $\langle j_0\rangle + c_2\langle j_2\rangle$. The ground state wavefunctions are given for an axis of quantization along the applied field.

**Table 2.** Comparison of the calculated intensities $I^{\text{calc}}$ with the observed intensities $I^{\text{obs}}$ (error $\sigma$).

| $(hkl)^{\pm}$ | $I^{\text{obs}}$ | $\sigma$ | $I^{\text{calc}}$ | $\Delta I/\sigma$ |
|---|---|---|---|---|
| $(000)^{+}$ | 35.22 | 1.66 | 33.41 | 1.09 |
| $(111)^{-}$ | 28.95 | 1.77 | 33.41 | −2.52 |
| $(002)^{-}$ | 149.61 | 4.26 | 143.10 | 1.53 |
| $(11\bar{1})^{-}$ | 155.53 | 5.70 | 143.10 | 2.18 |
| $(220)^{-}$ | 520.18 | 12.68 | 515.20 | 0.39 |
| $(11\bar{1})^{+}$ | 507.49 | 12.44 | 515.20 | −0.62 |
| $(222)^{-}$ | 3.77 | 4.03 | 1.68 | 0.52 |
| $(111)^{+}$ | 8.56 | 5.04 | 1.68 | 1.37 |
| $(002)^{+}$ | 57.49 | 7.39 | 55.89 | 0.22 |
| $(113)^{-}$ | 53.41 | 3.32 | 55.89 | −0.75 |
| $(22\bar{2})^{-}$ | 127.60 | 8.65 | 111.16 | 1.90 |
| $(11\bar{3})^{+}$ | 126.58 | 5.19 | 111.16 | 2.97 |
| $(331)^{-}$ | 222.11 | 8.23 | 205.33 | 2.04 |
| $(220)^{+}$ | 226.17 | 8.52 | 205.33 | 2.45 |
| $(004)^{-}$ | 556.09 | 13.71 | 560.41 | −0.32 |
| $(11\bar{3})^{-}$ | 575.09 | 15.02 | 560.41 | 0.98 |
| $(224)^{-}$ | 134.89 | 5.91 | 126.87 | 1.36 |
| $(113)^{+}$ | 135.45 | 6.72 | 126.87 | 1.28 |
| $(222)^{+}$ | 0.29 | 5.08 | 0.06 | 0.05 |
| $(333)^{-}$ | 8.96 | 6.09 | 0.06 | 1.46 |
| $(004)^{+}$ | 376.68 | 10.14 | 363.92 | 1.26 |
| $(115)^{-}$ | 387.63 | 12.69 | 363.92 | 1.87 |
| $(22\bar{4})^{-}$ | 382.82 | 9.98 | 410.08 | −2.73 |
| $(11\bar{5})^{+}$ | 382.41 | 11.77 | 410.08 | −2.35 |
| $(33\bar{3})^{-}$ | 358.15 | 9.74 | 393.45 | −3.62 |
| $(22\bar{4})^{+}$ | 363.26 | 13.47 | 393.45 | −2.24 |
| $(024)^{+}$ | 15.76 | 10.34 | 36.24 | −1.98 |
| $(442)^{-}$ | 13.67 | 8.40 | 17.02 | −0.40 |
| $(331)^{+}$ | 24.50 | 5.53 | 17.02 | 1.35 |
| $(135)^{-}$ | 22.39 | 5.04 | 32.36 | −1.98 |
| $(115)^{+}$ | 32.33 | 4.77 | 38.08 | −1.21 |
| $(226)^{-}$ | 36.61 | 5.08 | 38.08 | −0.29 |

## 3. Discussion

### *3.1. The magnetic form factor of a $\Gamma_7$ ground state*

The refinement of the $CeAl_2$ magnetic structure has been made possible only after having taken into account a detailed analysis of the Ce form factor. As already said, the former investigations in the paramagnetic state had shown that the Ce atom in $CeAl_2$ is in a $\Gamma_7$ ground level and therefore its form factor presents two characteristics: (i) it very much depends on the direction of the applied magnetic field, and (ii) it presents a very large scattering of the points instead of the usual continuous curve versus $\sin\theta/\lambda$, reflecting a strong anisotropy for the magnetization density.

Actually, the $\Gamma_7$ ground state is a linear combination of two almost degenerate wavefunctions (completely degenerate in the absence of a magnetic field). The form factor depends essentially on the direction of the applied magnetic field which gives rise to some corresponding magnetization density, even if the magnitude of the field is infinitesimal. To illustrate the importance of this feature, we have represented in figure 4 the magnetization density and the wavefunction of the ground state, once the degeneracy has been lifted by an infinitesimal field applied along the four-fold, two-fold and three-fold axes (the quantization axis $z$).

For this reason, for a magnetic structure without any field applied on the crystal, the magnetization density is aroused by the local molecular field in the direction of $\boldsymbol{m}^k$. In our compound, two Fourier components $\boldsymbol{m}^{k_1}$ and $\boldsymbol{m}^{k_2}$ are coupled and give rise to different magnetic satellites. One has then to consider separately the component of the molecular field associated with $\boldsymbol{k}_1$ (parallel to $\boldsymbol{m}^{k_1}$) and the component associated with $\boldsymbol{k}_2$ (parallel to $\boldsymbol{m}^{k_2}$). Considering the data treatment, one had to use a form factor for an applied field close to the adequate three-fold axis, and to check, by a self-consistent process, that the final direction of $\boldsymbol{m}^k$ is the same as the one taken to calculate the form factor used in the refinement. Let us emphasize once more that if the form factor depends in a very critical way on the direction of the applied field, it depends only slightly on the exact value of this field.

### *3.2. Comparison with the polarization analysis*

The refinement of the magnetic structure showed the existence of two angles, both expected by the symmetry analysis, and which are temperature dependent:

- the angle $\theta_{m^k}$, which measures the deviation of the Fourier vector $\boldsymbol{m}^k$ from the [111] direction, is related to the ratio $|m_z^k|/|m_x^k|$ of the moduli of $m_z^k$ and $m_x^k$. This angle is counted positive in the direction of [001], negative in the direction [110] and is null if $|m_x^k| = |m_z^k|$.
- the phase difference $\pm\varphi$ between components $m_x^k$ or $m_y^k$ and component $m_z^k$.

Both angles were anticipated by the symmetry analysis and their magnitudes are determined, not by the symmetries, but by the values of the exchange integrals. They were both found to be small, but still significant. Their variation with temperature below $T_N$ is very coherent and compares well with the spherical polarization analysis experiment [2]. In that experiment, the initial polarization is successively set 'up' ($P_{\text{up}}$ vertical), 'left' ($P_{\text{left}}$ perpendicular to the scattering vector) and 'front' ($P_{\text{front}}$ parallel to the scattering vector). The $CeAl_2$ crystal was aligned with the $[2\overline{11}]$ axis vertical and the rotation of the final polarization was determined after scattering from the $(1/2, -3/2 + \delta, 5/2 - \delta)$ reflection. As the temperature decreased from $T_N$ down to 1.15 K, deviations from the rotations expected for $\boldsymbol{m}^k$ aligned along [111] were found: the rotation of $P_{\text{up}}$ changed from 180° to 176 ± 0.5°, that of $P_{\text{left}}$ changed from 0° to 5 ± 0.5°, whereas that of $P_{\text{front}}$ remained unchanged at 180°. These deviations from 180° or 0° (4 ± 0.5° and 5 ± 0.5°, respectively for $\Delta T = 2.65$ *K*) are representative of the small angle $\theta_{m^k}$ (linear effect) and not of the small phase $\varphi$ (quadratic effect). With the values of $\theta_{m^k}$ found in our structure refinements (present paper), one can calculate between 1.3 and 3.52 K ($\Delta T = 2.22$ K) deviations of 3.1° ± 1.2° for $P_{\text{up}}$ and $P_{\text{left}}$. The agreement with the polarization analysis experiment is quite satisfactory.

### *3.3. Magnetic moments in the real space*

The magnetic moments for the two sites $Ce_1$ and $Ce_2$ located in a cell $\boldsymbol{l}$ (with $l_x$, $l_y$, and $l_z$ being integers or half integers in the fcc unit cell) can be written as follows.

- If the magnetic structure were single-$\boldsymbol{k}$:

$$\begin{aligned} \boldsymbol{m}_1(\boldsymbol{l}) &= \boldsymbol{m}_1^k \mathrm{e}^{-2\mathrm{i}\pi \boldsymbol{k}\cdot\boldsymbol{l}} + \mathrm{cc} \\ \boldsymbol{m}_2(\boldsymbol{l}) &= \boldsymbol{m}_2^k \mathrm{e}^{-2\mathrm{i}\pi \boldsymbol{k}\cdot\boldsymbol{l}} + \mathrm{cc} \end{aligned} \tag{6}$$

  where, according to relations (3) for the Fourier vector $\boldsymbol{m}_j^k$, there is a phase difference $\pm\varphi$ of the components $m_x^k$ and $m_y^k$ relative to the component $m_z^k$. This would involve $m_{jx}(\boldsymbol{l})$ and $m_{jy}(\boldsymbol{l})$ being no longer exactly equal, resulting, as $\varphi$ is very small, in a slight non-colinearity of the corresponding sinusoid.
- In the case of the double-$\boldsymbol{k}$ structure of $CeAl_2$, the moments are the sum of the Fourier contributions due to $\boldsymbol{k}_1$ and to $\boldsymbol{k}_2$. Taking into account the fact that the magnetic domains are twice as large as in the case of the single-$\boldsymbol{k}$ structure, the moments can be written as:

$$\begin{aligned} \boldsymbol{m}_1(\boldsymbol{l}) &= (1/\sqrt{2})(\boldsymbol{m}_1^{k_1} \mathrm{e}^{-2\mathrm{i}\pi \boldsymbol{k}_1\cdot\boldsymbol{l}} + \boldsymbol{m}_1^{k_2} \mathrm{e}^{-2\mathrm{i}\pi \boldsymbol{k}_2\cdot\boldsymbol{l}} + \mathrm{cc}) \\ \boldsymbol{m}_2(\boldsymbol{l}) &= (1/\sqrt{2})(\boldsymbol{m}_2^{k_1} \mathrm{e}^{-2\mathrm{i}\pi \boldsymbol{k}_1\cdot\boldsymbol{l}} + \boldsymbol{m}_2^{k_2} \mathrm{e}^{-2\mathrm{i}\pi \boldsymbol{k}_2\cdot\boldsymbol{l}} + \mathrm{cc}). \end{aligned} \tag{7}$$

There is an extra phase difference $\omega$ between the two Fourier vectors $\boldsymbol{m}^{k_1}$ and $\boldsymbol{m}^{k_2}$, which cannot be measured by the experiment. Taking into account the fact that $\boldsymbol{k}_1 = (k_{1x}, k_{1y}, k_{1z})$ and $\boldsymbol{k}_2 = (k_{1x}, k_{1y}, -k_{1z})$, the components of the $\boldsymbol{m}_j^{k_i}$ are the following; for the $Ce_1$ atom:

$$\begin{aligned} m_{1x}^{k_1} &= |m_x^k| \mathrm{e}^{\mathrm{i}\varphi} \mathrm{e}^{-\mathrm{i}\omega/2} & m_{1x}^{k_2} &= |m_x^k| \mathrm{e}^{\mathrm{i}\varphi} \mathrm{e}^{\mathrm{i}\omega/2} \\ m_{1y}^{k_1} &= |m_x^k| \mathrm{e}^{-\mathrm{i}\varphi} \mathrm{e}^{-\mathrm{i}\omega/2} & m_{1y}^{k_2} &= |m_x^k| \mathrm{e}^{-\mathrm{i}\varphi} \mathrm{e}^{\mathrm{i}\omega/2} \\ m_{1z}^{k_1} &= |m_z^k| \mathrm{e}^{-\mathrm{i}\omega/2} & m_{1z}^{k_2} &= -|m_z^k| \mathrm{e}^{\mathrm{i}\omega/2} \end{aligned}$$

and for the $Ce_2$ atom:

$$\begin{aligned} m_{2x}^{k_1} &= -|m_x^k| \mathrm{e}^{-\mathrm{i}\varphi} \mathrm{e}^{-\mathrm{i}\omega/2} & m_{2x}^{k_2} &= |m_x^k| \mathrm{e}^{-\mathrm{i}\varphi} \mathrm{e}^{\mathrm{i}\omega/2} \\ m_{2y}^{k_1} &= -|m_x^k| \mathrm{e}^{\mathrm{i}\varphi} \mathrm{e}^{-\mathrm{i}\omega/2} & m_{2y}^{k_2} &= |m_x^k| \mathrm{e}^{\mathrm{i}\varphi} \mathrm{e}^{\mathrm{i}\omega/2} \\ m_{2z}^{k_1} &= -|m_z^k| \mathrm{e}^{-\mathrm{i}\omega/2} & m_{2z}^{k_2} &= -|m_z^k| \mathrm{e}^{\mathrm{i}\omega/2} \end{aligned}$$

and, as $k_{1x} = 1/2 + \delta$, $k_{1y} = 1/2 - \delta$ and $k_{1z} = 1/2$, the components of the moments on $Ce_1$ and $Ce_2$ are given by the following; for the $Ce_1$ atom:

$$\begin{aligned} m_{1x}(\boldsymbol{l}) &= (4/\sqrt{2})|m_x^k| \cos(\pi l_0 - \varphi) \cos(\pi l_z + \omega/2) \\ m_{1y}(\boldsymbol{l}) &= (4/\sqrt{2})|m_x^k| \cos(\pi l_0 + \varphi) \cos(\pi l_z + \omega/2) \\ m_{1z}(\boldsymbol{l}) &= -(4/\sqrt{2})|m_z^k| \sin(\pi l_0) \sin(\pi l_z + \omega/2) \end{aligned}$$

and for the $Ce_2$ atom:

$$\begin{aligned} m_{2x}(\boldsymbol{l}) &= (4/\sqrt{2})|m_x^k| \sin(\pi l_0 + \varphi) \sin(\pi l_z + \omega/2) \\ m_{2y}(\boldsymbol{l}) &= (4/\sqrt{2})|m_x^k| \sin(\pi l_0 - \varphi) \sin(\pi l_z + \omega/2) \\ m_{2z}(\boldsymbol{l}) &= -(4/\sqrt{2})|m_z^k| \cos(\pi l_0) \cos(\pi l_z + \omega/2) \end{aligned}$$

with $l_0 = (l_x + l_y) + 2\delta(l_x - l_y)$.

The most probable value of $\omega$ is $\pi/2$ as it allows the magnetic moments of the $Ce^{3+}$ Kramers ion not to vanish with the propagation and to behave in the same way on the two cerium sites. Such a phase is also consistent with the fourth-order terms in the free energy [7]. The values found for $\varphi$ are small and change from positive to negative as temperature decreases. For $\varphi = 0$, $m_{jx}(\boldsymbol{l}) = m_{jy}(\boldsymbol{l})$ for both atoms $Ce_1$ and $Ce_2$. The corresponding magnetic structure is described by two equivalent elliptical helices with opposed chiralities. For $\varphi \neq 0$, the moments are no longer exactly in the bisecting $(1\overline{1}0)$ plane. The elliptical helices are slightly distorted, with a shift of the moment away from that plane. As $\varphi$ is very small at all temperatures, this distortion remains very weak.

## 4. Conclusion

The achievement of the $CeAl_2$ magnetic structure determination by neutron diffraction on a single crystal has been a long and rather delicate piece of work. There were experimental difficulties connected with the instrumental resolution needed to obtain clean and unpolluted magnetic reflection intensities. There were difficulties in the data treatment due to a very unusual magnetic form factor, a form factor which strongly depends on the direction of the Fourier components of the magnetic moments. There was also the delicate question of the existence of a phase difference between the $x$, $y$ and $z$ projections of these Fourier components. It is important to be able to conclude that this phase difference does exist and varies with

temperature, even if it has been found to be very small. We think that we now have a magnetic structure which goes along with the theory and fits well with a good quality set of neutron data.

## Acknowledgments

The authors would like to thank J Villain and A B Harris for very fruitful discussions on the symmetry analysis of the $CeAl_2$ magnetic structure and A Buhot for his help with the graphical representation of the magnetization density of the $\Gamma_7$ ground state.

## Appendix. Calculation of the magnetic form factor

The magnetic form factor $f(\boldsymbol{\kappa})$ associated with the moment $\mu$ and the wavefunction

$$|\psi\rangle = \sum_M a_M |JM\rangle$$

of each energy level is deduced from the relation giving the $q$th spherical components of the interaction operator $\hat{\mathbf{Q}}_\perp(\boldsymbol{\kappa})$ [16]:

$$E_q = (\mu f(\boldsymbol{\kappa})_\perp)_q = \langle\psi|\hat{\mathbf{Q}}_\perp(\boldsymbol{\kappa})_q|\psi\rangle \qquad \text{(A.1)}$$

with

$$\langle JM|\hat{\mathbf{Q}}_\perp(\boldsymbol{\kappa})_q|JM'\rangle = (4\pi)^{1/2}\sum_{KK'}\{A_J(K,K') + B_J(K,K')\} \times \sum_{QQ'} Y_K^Q(\widetilde{\boldsymbol{\kappa}})\langle K'Q'JM'|JM\rangle\langle KQK'Q'|1q\rangle \qquad \text{(A.2)}$$

where $A_J(K,K')$ and $B_J(K,K')$, which are linear combinations of the radial integrals $\langle j_K(\kappa)\rangle$ [12], are the orbital and spin contributions respectively. $\langle K'Q'JM'|JM\rangle$ and $\langle KQK'Q'|1q\rangle$ are Clebsch–Gordan coefficients and $Y_K^Q(\widetilde{\boldsymbol{\kappa}})$ a spherical harmonic. The component $q = 0$ refers to the $z$ component and $q = \pm 1$ to the components $x \pm \mathrm{i}y$.

In usual magnetic form factor measurements, the scattering amplitude $\mu f$ is measured along a direction $z$ almost perpendicular to the scattering vector $Q$ ($\alpha \simeq \pi/2$). Generally, only the term $E_0 = (\mu f_\perp)_z$ is considered [17] and in this case one uses $\mu f = (\mu f_\perp)_z/\sin^2\alpha$.

For our calculation, the scattering vector $Q$ points along all the directions of space and, for some reflections, even close to the direction of $F_M$. We preferred to consider also the terms $E_1$ and $E_{-1}$ which lead to $(\mu f_\perp)_x$ and $(\mu f_\perp)_y$. The value of the form factor is then obtained by the exact formula $\mu f = |\mu f_\perp|/\sin\alpha$.

## References

[1] Barbara B, Boucherle J-X, Buevoz J-L, Rossignol M F and Schweizer J 1977 *Solid State Commun.* **24** 481
Barbara B, Boucherle J-X, Buevoz J-L, Rossignol M F and Schweizer J 1979 *Solid State Commun.* **29** 810
[2] Givord F, Schweizer J and Tasset F 1997 *Physica* B **234–236** 685
[3] Barbara B, Rossignol M F, Boucherle J-X, Schweizer J and Buevoz J-L 1979 *J. Appl. Phys.* **50** 2300
[4] Barbara B, Rossignol M F, Boucherle J-X and Vettier C 1980 *Phys. Rev. Lett.* **45** 938
[5] Shapiro S M, Gurewitz E, Parks R D and Kupferberg L C 1979 *Phys. Rev. Lett.* **43** 1748
[6] Forgan E M, Rainford B D, Lee S L, Abell J S and Bi Y 1990 *J. Phys.: Condens. Matter* **2** 10211
[7] Harris A B and Schweizer J 2006 *Phys. Rev.* B **74** 134411
[8] Schweizer J 2001 *J. Physique* IV **11** Pr9–105
[9] Schweizer J, Villain J and Harris A B 2007 *Eur. Phys. J. Appl. Phys.* **38** 41
[10] Schweizer J 2006 *C. R. Physique* **7** 823
[11] Wolfers P 1990 *J. Appl. Crystallogr.* **23** 554
[12] Freeman A J and Desclaux J-P 1979 *J. Magn. Magn. Mater.* **12** 11
[13] Lander G H and Brun T O 1970 *J. Chem. Phys.* **53** 1387
[14] Boucherle J-X and Schweizer J 1985 *Physica* B **130** 337
[15] Thalmeier P and Fulde P 1982 *Phys. Rev. Lett.* **49** 1588
[16] Lovesey S W 1984 *Theory of Neutron Scattering from Condensed Matter* (Oxford: Oxford University Press)
[17] Boucherle J-X and Schweizer J 1981 *J. Magn. Magn. Mater.* **24** 308